JHEP 1311 (2013) 211
arXiv:1309.3192 [hep-ph]

Light Sterile Neutrinos in Cosmology and Short-Baseline Oscillation Experiments

S. Gariazzo
Department of Physics, University of Torino, and INFN, Sezione di Torino, Via P. Giuria 1, I–10125 Torino, Italy

C. Giunti
INFN, Sezione di Torino, and Department of Physics, University of Torino, Via P. Giuria 1, I–10125 Torino, Italy

M. Laveder
Dipartimento di Fisica e Astronomia "G. Galilei", Università di Padova, and INFN, Sezione di Padova, Via F. Marzolo 8, I–35131 Padova, Italy

arXiv:1309.3192v2 [hep-ph] 19 Feb 2014

We analyze the most recent cosmological data, including Planck, taking into account the possible existence of a sterile neutrino with a mass at the eV scale indicated by short-baseline neutrino oscillations data in the 3+1 framework. We show that the contribution of local measurements of the Hubble constant induces an increase of the value of the effective number of relativistic degrees of freedom above the Standard Model value, giving an indication in favor of the existence of sterile neutrinos and their contribution to dark radiation. Furthermore, the measurements of the local galaxy cluster mass distribution favor the existence of sterile neutrinos with eV-scale masses, in agreement with short-baseline neutrino oscillations data. In this case there is no tension between cosmological and short-baseline neutrino oscillations data, but the contribution of the sterile neutrino to the effective number of relativistic degrees of freedom is likely to be smaller than one. Considering the Dodelson-Widrow and thermal models for the statistical cosmological distribution of sterile neutrinos, we found that in the Dodelson-Widrow model there is a slightly better compatibility between cosmological and short-baseline neutrino oscillations data and the required suppression of the production of sterile neutrinos in the early Universe is slightly smaller.

PACS numbers: 14.60.Pq, 14.60.Lm, 14.60.St, 98.80.-k

I. INTRODUCTION

The recent results of the Planck experiment [1, 2] generated lively discussions [3–14] on the value of the effective number of relativistic degrees of freedom $N_{\rm eff}$ before photon decoupling (see [15–17]), which gives the energy density of radiation ρ_R through the relation

$$\rho_R = \left[1 + \frac{7}{8}\left(\frac{4}{11}\right)^{4/3} N_{\rm eff}\right] \rho_\gamma, \tag{1}$$

where ρ_γ is the photon energy density. Since the value of $N_{\rm eff}$ in the Standard Model (SM) is $N_{\rm eff}^{\rm SM} = 3.046$ [18, 19], a positive measurement of $\Delta N_{\rm eff} = N_{\rm eff} - N_{\rm eff}^{\rm SM}$ may be a signal that the radiation content of the universe was due not only to photons and SM neutrinos, but also to some additional light particle called generically "dark radiation".

In this paper we consider the possiblity that the dark radiation is made of the light sterile neutrinos (see [20–23]) whose existence is indicated by recent results of short-baseline (SBL) neutrino oscillation experiments [24–30]. In particular, we consider the simplest possibility of a 3+1 scheme, in which the three active flavor neutrinos ν_e, ν_μ, ν_τ, are mainly composed of three very light neutrinos ν_1, ν_2, ν_3, with masses much smaller than 1 eV and there is a sterile neutrino ν_s which is mainly composed of a new massive neutrino ν_4 with mass $m_4 \sim 1\,\text{eV}$.

The problem of the determination of $N_{\rm eff}$ from cosmological data is related to that of the Hubble constant H_0, because these two quantities are positively correlated in the analysis of the data (see Refs. [31, 32]). Since dedicated local astrophysical experiments obtained values of H_0 which are larger than that obtained by the Planck collaboration from the analysis of cosmological data alone [2], there is an indication that $N_{\rm eff}$ may be larger than the SM value. We discuss this problem in Section II, where we present the results of a fit of cosmological data with a prior on H_0 determined by the weighted average of the local astrophysical measurements.

Since the neutrino oscillation explanation of SBL data requires the existence of a massive neutrino at the eV scale, we discuss also the bounds on the effective sterile neutrino mass $m_s^{\rm eff}$ defined by the Planck collaboration as [2]

$$m_s^{\rm eff} = (94.1\,\text{eV})\,\Omega_s h^2\,, \tag{2}$$

where $\Omega_s = \rho_s/\rho_c$ and h is the reduced Hubble constant, such that $H_0 = 100\,h\,\text{km}\,\text{s}^{-1}\,\text{Mpc}^{-1}$. Here ρ_s is the current energy density of $\nu_s \simeq \nu_4$ with mass $m_s \simeq m_4 \sim 1\,\text{eV}$ and ρ_c is the current critical density. The constant in Eq. (2) refers to a Fermi-Dirac distribution with the standard neutrino temperature $T_\nu = (4/11)^{1/3} T_\gamma$. We consider the two cases discussed by the Planck collaboration [2] (see also [33]):

Thermal (TH) model: The sterile neutrino has a

Fermi-Dirac distribution $f_s(E) = (e^{E/T_s}+1)^{-1}$ with a temperature T_s which is different from the temperature T_ν of the active neutrinos, leading to

$$m_s^{\rm eff} = (T_s/T_\nu)^3 m_s = (\Delta N_{\rm eff})^{3/4} m_s \,. \quad (3)$$

Dodelson-Widrow (DW) model: The sterile neutrino has a Fermi-Dirac distribution $f_s(E) = \chi_s/(e^{E/T_\nu}+1)$, with the same temperature T_ν as the active neutrinos but multiplied by a constant scale factor χ_s [34]. In this case

$$m_s^{\rm eff} = \chi_s \, m_s = \Delta N_{\rm eff} \, m_s \,. \quad (4)$$

A further important problem is the compatibility of the cosmological bounds on $N_{\rm eff}$ and $m_s^{\rm eff}$ with the active-sterile neutrino mixing required to fit SBL oscillation data. The stringent bounds on $N_{\rm eff}$ and $m_s^{\rm eff}$ presented in Ref. [2] by the Planck collaboration imply [35] that the production of sterile neutrinos in the early Universe is suppressed by some non-standard mechanism, as, for example, a large lepton asymmetry [36–39]. In this paper we adopt a phenomenological approach similar to that in Refs. [40–42]: we use the results of the fit of SBL neutrino oscillation data as a prior for the analysis of cosmological data. In this way, in Section III we derive the combined constraints on $N_{\rm eff}$ and $m_s^{\rm eff}$ and the related constraints on H_0 and m_s.

II. COSMOLOGICAL DATA AND LOCAL H_0 MEASUREMENTS

For our cosmological analysis we used a modified version of the publicly available software `CosmoMC`[1] [45] (March 2013 version), a Monte Carlo Markov Chain (MCMC) software which computes the theoretical predictions using CAMB[2] [46]. We used the following data sets and likelihood calculators:

- The recent Planck data [1] and likelihood codes [47] `CamSpec`, that computes the Planck TT likelihood[3] for the multipoles with $50 \leq l \leq 2500$, and `Commander`, that computes the low-l TT Planck likelihood. We will refer to this set as "Planck".
- The nine-year large-scale E-polarization WMAP data [48], included in the `CosmoMC` code through the downloadable likelihood data and code released by the Planck Collaboration. We will refer to this dataset as "WP".
- High-l spectra from Atacama Cosmology Telescope (ACT) [49] and South Pole Telescope (SPT) [50, 51] and the likelihood code[4] described in [52], which is based on WMAP likelihood code [53]. We will refer to this set as "highL" and to the Planck+WP+highL dataset as "CMB".
- Baryonic Acoustic Oscillations (BAO) [54] data. We used the BAO measurement at $z_{\rm eff} = 0.2$ and $z_{\rm eff} = 0.35$ from the Sloan Digital Sky Survey (SDSS) Data Release 7 (DR7) [55] galaxy catalogue, analyzed in [56] and [57], BAO measurement at $z_{\rm eff} = 0.57$ obtained from the SDSS Baryon Oscillation Spectroscopic Survey (BOSS) Data Release 9 (DR9) [58] galaxy catalogue, analyzed in [59], and the measurement at $z_{\rm eff} = 0.1$ obtained in [60] using data from the 6dF Galaxy Survey (6dFGS) [61]. We will refer to this set as "BAO".

TABLE I. Global best-fit value $H_0^{\rm gbf}$, marginal best-fit $H_0^{\rm mbf} \pm 1\sigma$ (68.27%) and 2σ (95.45%) limits for H_0 obtained from the analysis of the indicated data sets.

	data	$H_0^{\rm gbf}$	$H_0^{\rm mbf} \pm 1\sigma$	2σ
no SBL prior	CMB+H_0	73.6	$72.7^{+1.9}_{-1.7}$	69.0 ÷ 76.3
	CMB+H_0+BAO	71.1	$71.5^{+1.4}_{-1.4}$	68.7 ÷ 74.4
	CMB+H_0+BAO+LGC	71.1	$70.4^{+1.5}_{-1.3}$	68.1 ÷ 73.5
TH SBL prior	CMB	66.8	$66.6^{+1.1}_{-1.2}$	64.3 ÷ 68.9
	CMB+H_0	68.7	$68.7^{+1.0}_{-1.1}$	66.5 ÷ 70.7
	CMB+H_0+BAO	68.7	$68.8^{+0.8}_{-0.7}$	67.3 ÷ 70.4
	CMB+H_0+BAO+LGC	69.1	$69.3^{+0.6}_{-0.6}$	68.1 ÷ 70.6
DW SBL prior	CMB	66.5	$66.9^{+1.2}_{-1.3}$	64.6 ÷ 69.4
	CMB+H_0	68.1	$68.9^{+1.1}_{-1.0}$	66.9 ÷ 71.0
	CMB+H_0+BAO	69.3	$69.1^{+0.8}_{-0.8}$	67.6 ÷ 70.6
	CMB+H_0+BAO+LGC	69.5	$69.7^{+0.7}_{-0.5}$	68.6 ÷ 71.0

TABLE II. Global best-fit value $N_{\rm eff}^{\rm gbf}$, marginal best-fit $N_{\rm eff}^{\rm mbf} \pm 1\sigma$ (68.27%) and 2σ (95.45%) limits for $N_{\rm eff}$ obtained from the analysis of the indicated data sets.

	data	$N_{\rm eff}^{\rm gbf}$	$N_{\rm eff}^{\rm mbf} \pm 1\sigma$	2σ
no SBL prior	CMB+H_0	3.84	$3.76^{+0.25}_{-0.23}$	3.29 ÷ 4.26
	CMB+H_0+BAO	3.59	$3.71^{+0.23}_{-0.27}$	3.17 ÷ 4.18
	CMB+H_0+BAO+LGC	3.57	$3.51^{+0.29}_{-0.29}$	3.05 ÷ 4.01
TH SBL prior	CMB	3.29	$3.26^{+0.21}_{-0.10}$	3.05 ÷ 3.67
	CMB+H_0	3.23	$3.23^{+0.19}_{-0.12}$	3.05 ÷ 3.66
	CMB+H_0+BAO	3.11	$3.23^{+0.15}_{-0.11}$	3.05 ÷ 3.55
	CMB+H_0+BAO+LGC	3.36	$3.32^{+0.12}_{-0.09}$	3.15 ÷ 3.57
DW SBL prior	CMB	3.43	$3.35^{+0.16}_{-0.15}$	3.09 ÷ 3.73
	CMB+H_0	3.19	$3.31^{+0.18}_{-0.13}$	3.08 ÷ 3.70
	CMB+H_0+BAO	3.29	$3.30^{+0.13}_{-0.13}$	3.08 ÷ 3.60
	CMB+H_0+BAO+LGC	3.30	$3.42^{+0.11}_{-0.11}$	3.22 ÷ 3.67

[1] `http://cosmologist.info/cosmomc/`

[2] `http://camb.info/`

[3] `http://pla.esac.esa.int/pla/aio/planckProducts.html`

[4] `http://lambda.gsfc.nasa.gov/product/act/act_fulllikelihood_get.cfm`

TABLE III. Global best-fit value $m^{\rm eff}_{s,\rm gbf}$, marginal best-fit value $m^{\rm eff}_{s,\rm mbf}$, 1σ (68.27%) and 2σ (95.45%) intervals for $m^{\rm eff}_{s}$ in eV obtained from the analysis of the indicated data sets without and with the SBL prior in the thermal (TH) and Dodelson-Widrow (DW) models. We give also the corresponding quantities for m_s.

	data	$m^{\rm eff}_{s,\rm gbf}$	$m^{\rm eff}_{s,\rm mbf}$	1σ	2σ	$m^{\rm gbf}_{s}$	$m^{\rm mbf}_{s}$	1σ	2σ	
no SBL prior	CMB+H_0	0	0	< 0.10	< 0.27	0	0	< 0.13	< 0.38	(TH)
								< 0.14	< 0.44	(DW)
	CMB+H_0+BAO	0	0	< 0.13	< 0.32	0	0	< 0.18	< 0.51	(TH)
								< 0.21	< 0.65	(DW)
	CMB+H_0+BAO+LGC	0.41	0.42	$0.28 \div 0.56$	$0.15 \div 0.70$	0.67	0.62	$0.21 \div 1.14$	$0.00 \div 2.68$	(TH)
						0.79	0.92	$0.00 \div 1.11$	$0.00 \div 4.81$	(DW)
TH SBL prior	CMB	0.45	0.42	$0.26 \div 0.67$	$0.11 \div 0.89$	1.30	1.28	$1.09 \div 1.36$	$0.96 \div 1.42$	
	CMB+H_0	0.35	0.38	$0.20 \div 0.61$	$0.05 \div 0.86$	1.28	1.28	$1.08 \div 1.35$	$0.95 \div 1.40$	
	CMB+H_0+BAO	0.17	0.37	$0.20 \div 0.54$	$0.08 \div 0.75$	1.29	1.27	$1.08 \div 1.35$	$0.95 \div 1.39$	
	CMB+H_0+BAO+LGC	0.47	0.48	$0.35 \div 0.60$	$0.25 \div 0.74$	1.12	1.27	$1.08 \div 1.35$	$0.95 \div 1.40$	
DW SBL prior	CMB	0.44	0.36	$0.19 \div 0.57$	$0.06 \div 0.83$	1.13	1.28	$1.08 \div 1.35$	$0.96 \div 1.42$	
	CMB+H_0	0.16	0.35	$0.16 \div 0.53$	$0.04 \div 0.77$	1.13	1.28	$1.07 \div 1.35$	$0.94 \div 1.39$	
	CMB+H_0+BAO	0.32	0.28	$0.16 \div 0.46$	$0.06 \div 0.64$	1.28	1.27	$1.07 \div 1.34$	$0.95 \div 1.39$	
	CMB+H_0+BAO+LGC	0.32	0.45	$0.33 \div 0.58$	$0.22 \div 0.72$	1.27	1.28	$1.08 \div 1.35$	$0.95 \div 1.40$	
	SBL [30]					1.27	1.27	$1.10 \div 1.36$	$0.97 \div 1.42$	

- Local Galaxy Cluster data from the Chandra Cluster Cosmology Project [62] observations, from which the cluster mass distribution at low and high redshift is calculated. The likelihood has been presented in [63] and a `CosmoMC` module is publicly available[5]. We will refer to this set as "LGC".

The analysis of Planck+WP+highL data performed by the Planck collaboration in the framework of the standard ΛCDM cosmological model gave for the Hubble constant the value (see Eq. (51) of Ref. [2])

$$H_0 = 67.3 \pm 1.2\,\mathrm{km\,s^{-1}\,Mpc^{-1}}\,. \tag{5}$$

This value has a remarkable tension with the results of recent direct local astrophysical measurements of H_0, which found significantly higher values. Here we consider the following two compatible measurements:

Cepheids+SNe Ia: Hubble Space Telescope (HST) observations of Cepheid variables in the host galaxies of eight SNe Ia have been used to calibrate the supernova magnitude-redshift relation, leading to [43]

$$H_0 = 73.8 \pm 2.4\,\mathrm{km\,s^{-1}\,Mpc^{-1}}\,. \tag{6}$$

This value is in agreement with the result $H_0 = 74.3 \pm 2.6\,\mathrm{km\,s^{-1}\,Mpc^{-1}}$ obtained in the Carnegie Hubble Program (Carnegie HP) [64] through a recalibration of the secondary distance methods used in the HST Key Project. We do not use the Carnegie Hubble Program value of H_0, because there is an overlap between the HST and Carnegie HP sets of SNe Ia data that induces a correlation in the statistical part of the uncertainty which is unknown to us.

COSMOGRAIL: Strong gravitational lensing time delay measurements of the system RXJ1131-1231, observed as part of the COSmological MOnitoring of GRAvitational Lenses (COSMOGRAIL) project, led to [44]:

$$H_0 = 78.7 \pm 4.5\,\mathrm{km\,s^{-1}\,Mpc^{-1}}\,. \tag{7}$$

Combining these local astrophysical measurements of H_0, we obtained the local weighted average

$$H_0 = 74.9 \pm 2.1\,\mathrm{km\,s^{-1}\,Mpc^{-1}}\,. \tag{8}$$

Since this value differs from that in Eq. (5) by about 3.1σ, there is a tension between the CMB and local determinations of H_0. One can see this tension also from the graphical representation of Eqs. (5)–(8) in the upper-right panel of Fig. 1.

Let us emphasize however that the Planck value of H_0 in Eq. (5) has been obtained assuming the standard ΛCDM cosmological model in which $N_{\rm eff}$ is assumed to have the SM value $N_{\rm eff}^{\rm SM}$. Since H_0 and $N_{\rm eff}$ are positively correlated (see Refs. [31, 32]), one can expect that leaving $N_{\rm eff}$ free the tension is reduced. Indeed, from the analysis of CMB data without constraints on $N_{\rm eff}$ the Planck collaboration obtained[6]

$$H_0 = 69.7 \pm 2.8\,\mathrm{km\,s^{-1}\,Mpc^{-1}}\,. \tag{9}$$

Hence, the tension of CMB Planck data with the local weighted average value of H_0 in Eq. (8) almost disappears when $N_{\rm eff}$ is not constrained to its SM value. Hence, we performed a fit of cosmological data with a Gaussian prior for H_0 having mean and standard deviation given by the local average in Eq. (8). In the following we refer to this prior as "H_0".

Since we are interested in studying the effect on the analysis of cosmological data of a sterile neutrino mass motivated by SBL oscillation anomalies, we consider an extension of the standard cosmological model in which both $N_{\rm eff}$ and $m_s^{\rm eff}$ are free parameters to be determined by the fit of the data.

Figure 1 and the first parts of Tabs. I, II and III shows the results for H_0, $N_{\rm eff}$ and $m_s^{\rm eff}$ obtained from the fits of CMB, CMB+H_0, CMB+H_0+BAO and CMB+H_0+BAO+LGC data. In Tab. III we give also the corresponding results for $m_s \simeq m_4$, which depends on the statistical distribution of sterile neutrinos. Therefore, we distinguish the results for m_s obtained in the thermal (TH) and Dodelson-Widrow (DW) models using, respectively, Eqs. (3) and (4). In Figs. 2, 3 and 4 we compare graphically the allowed ranges of $N_{\rm eff}$, $m_s^{\rm eff}$ and m_s obtained in the different fits.

From the bottom-left panel in Fig. 1, one can see that the fit of CMB data alone restricts $m_s^{\rm eff}$ to small values only for $N_{\rm eff} \gtrsim 3.2$, whereas there is a tail of allowed large values of $m_s^{\rm eff}$ for smaller $N_{\rm eff}$. This is in agreement with Fig. 28-right of Ref. [2], where it has been explained as corresponding to the case in which the sterile neutrino behaves as warm dark matter, because its mass is large and it becomes non-relativistic well before recombination. This happens in both the thermal and Dodelson-Widrow models, as one can infer from Eqs. (3) and (4). The presence of this tail of the posterior distribution of $m_s^{\rm eff}$ implies that the posterior distributions of the fitted parameters depend on the arbitrary upper value chosen for $m_s^{\rm eff}$ in the `CosmoMC` runs (we chose $m_s^{\rm eff} < 5\,\mathrm{eV}$, whereas the Planck Collaboration chose $m_s^{\rm eff} < 3\,\mathrm{eV}$). Hence, we do not present in the tables the numerical results of the fit of CMB data alone, which suffer from this arbitrariness.

The addition of the local H_0 prior leads to an increase of $N_{\rm eff}$ which evicts the large-$m_s^{\rm eff}$ and small-$N_{\rm eff}$ region

[5] `http://hea.iki.rssi.ru/400d/cosm/`

[6] See page 148 of the tables with 68% limits available at `http://www.sciops.esa.int/wikiSI/planckpla/index.php?title=Cosmological_Parameters&instance=Planck_Public_PLA`.

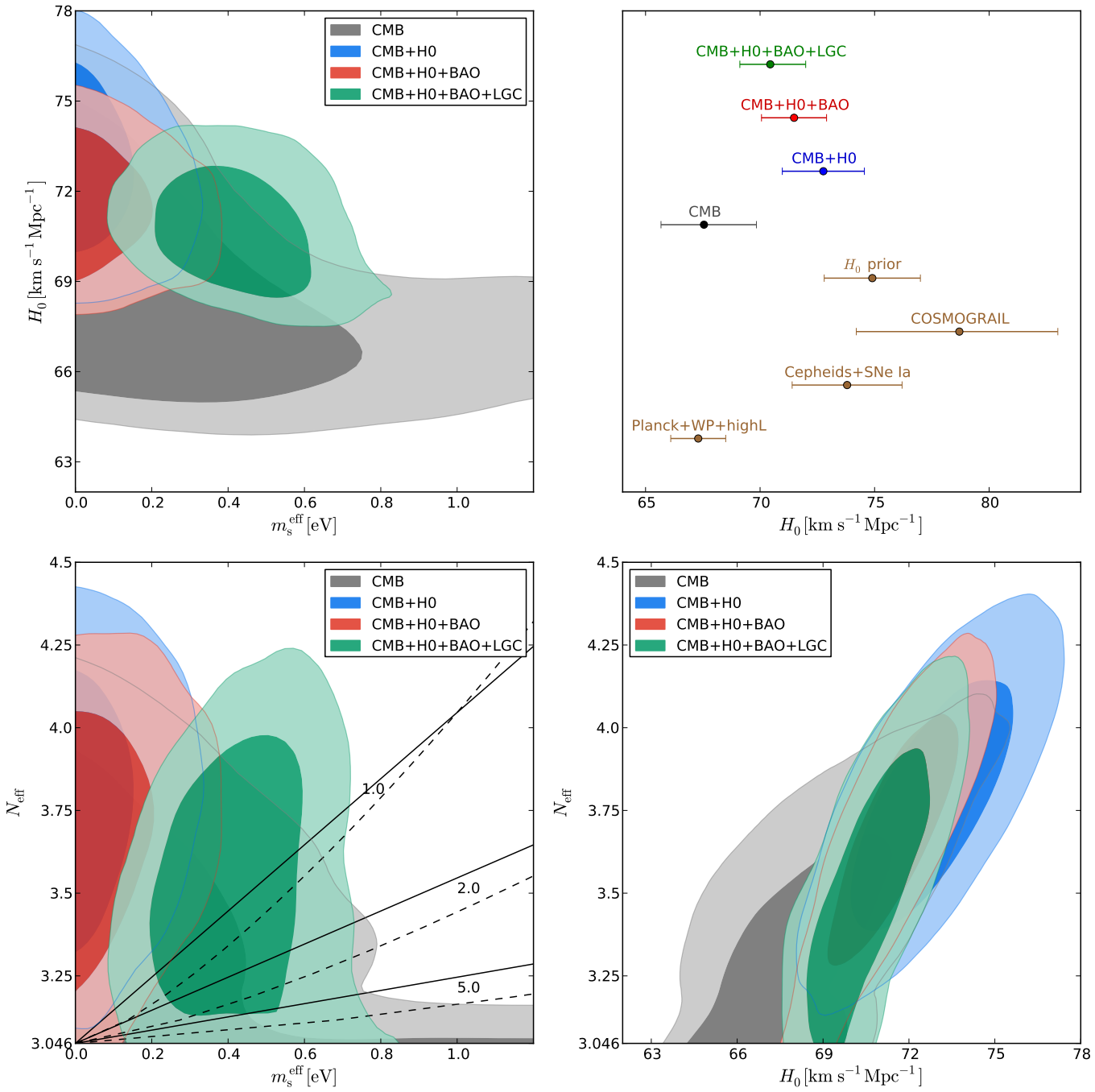


FIG. 1. Results of the analysis of cosmological data alone. The light and dark shadowed regions in the 2D plots show, respectively, the 68% and 95% marginalized posterior probability regions obtained from the analysis of the data sets indicated in the legends with corresponding color. In the bottom-left panel m_s is constant, with the indicated value in eV, along the dashed lines in the thermal model and along the solid lines in the Dodelson-Widrow model. The four lower intervals of H_0 in the upper-right panel correspond to: Eq. (5) for Planck+WP+highL [2], Eq. (6) for Cepheids+SNe Ia [43], Eq. (7) for COSMOGRAIL [44], Eq. (8) for the H_0 prior. In all panels the labels CMB, CMB+H_0, CMB+H_0+BAO and CMB+H_0+BAO+LGC indicate the fits performed in this work.

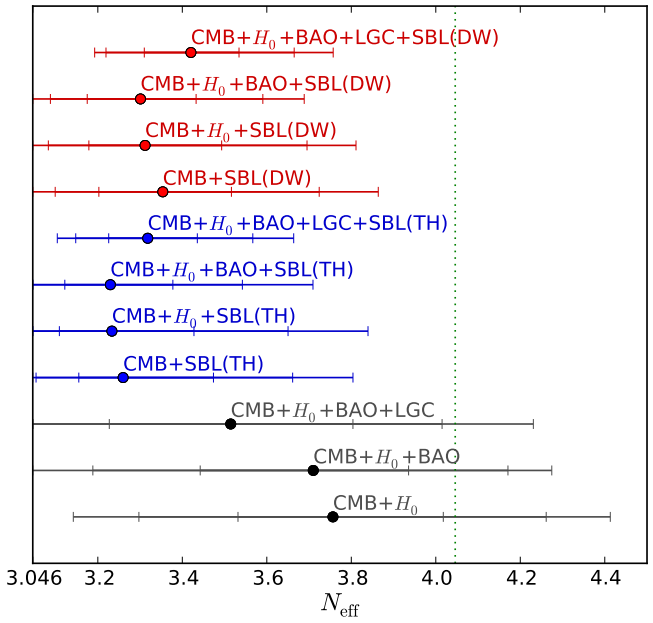


FIG. 2. Comparison of the allowed intervals of $N_{\rm eff}$ obtained from the fits of CMB, CMB+H_0, CMB+H_0+BAO and CMB+H_0+BAO+LGC data without (black) and with the SBL prior in the thermal (blue) and Dodelson-Widrow (red) models. The segments in each bar correspond to 68%, 95% and 99% probability. The dotted vertical line corresponds to $\Delta N_{\rm eff} = 1$.

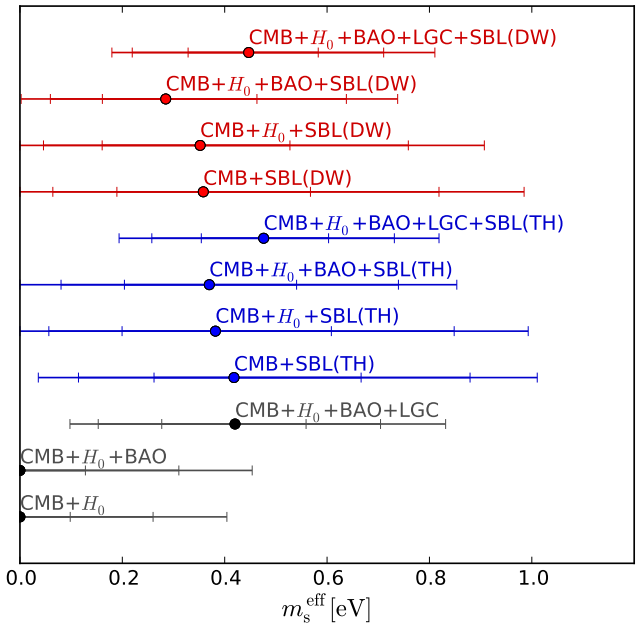


FIG. 3. Comparison of the allowed intervals of $m_s^{\rm eff}$ obtained from the fits of CMB, CMB+H_0, CMB+H_0+BAO and CMB+H_0+BAO+LGC data without (black) and with the SBL prior in the thermal (blue) and Dodelson-Widrow (red) models. The segments in each bar correspond to 68%, 95% and 99% probability.

in which the sterile neutrino behaves as cold dark matter. This can be seen from the CMB+H_0 allowed regions in Fig. 1 and the corresponding upper limits for $m_s^{\rm eff}$ and m_s in Figs. 3 and 4 and in Tab. III. The further addition of BAO data slightly lowers the best-fit values and allowed ranges of H_0 and $N_{\rm eff}$ (see Figs. 1 and 2 and Tabs. I and II). Hence, the upper limits for $m_s^{\rm eff}$ and m_s in Figs. 3 and 4 and in Tab. III are slightly larger, but still rather stringent, of the order of $m_s^{\rm eff} \lesssim 0.3\,{\rm eV}$ and $m_s \lesssim 0.6\,{\rm eV}$ at 2σ.

Comparing the CMB+H_0 and CMB+H_0+BAO allowed intervals of m_s in Tab. III and Fig. 4 with that obtained from the analysis of SBL data in the framework of 3+1 mixing [30], it is clear that there is a tension[7]: about 5.0σ, 4.6σ, 4.1σ, 3.5σ, respectively, in the CMB+H_0(TH), CMB+H_0(DW), CMB+H_0+BAO(TH) CMB+H_0+BAO(DW) fits. The tensions are smaller in the Dodelson-Widrow model and this could be an indication in favor of this case if SBL oscillations will be confirmed by future experiments (see Refs. [21, 68–74]).

Let us now consider the inclusion of the LGC data set in the cosmological fit. As discussed in Ref. [12], the measured amount of clustering of galaxies [62, 63] is smaller than that obtained by evolving the primordial density fluctuations with the relatively large matter density at recombination measured precisely by Planck [2]. The correlation of a relatively large matter density and clustering of galaxies can be quantified through the approximate relation $\sigma_8 \propto \Omega_m^{0.563}$ [75, 76] which relates the rms amplitude σ_8 of linear fluctuations today at a scale of $8h^{-1}\,{\rm Mpc}$ (where $h = H_0/100\,{\rm km\,s^{-1}\,Mpc^{-1}}$) with the present matter density Ω_m. As discussed in Ref. [12], the value of σ_8 and the amount of clustering of galaxies can be lowered by adding to the ΛCDM cosmological model hot dark matter in the form of sterile neutrinos with eV-scale masses[8]. The free-streaming of these sterile neutrinos suppresses the growth of structures which are smaller than the free-streaming length, leading to a suppression of σ_8 with respect to the ΛCDM approximate relation $\sigma_8 \propto \Omega_m^{0.563}$. In this way, the relatively large Planck value of Ω_m can be reconciled with the relatively small amount of local galaxy clustering in the LGC data set and the corresponding relatively small value of σ_8.

Hence, the inclusion of LGC data in the cosmological fits favors the existence of a sterile neutrino with a mass of the order of that required by SBL data, which is at least partially thermalized in the early Universe [12]. The results of our CMB+H_0+BAO+LGC fit given in

[7] Possible ways of solving this tension have been discussed recently, but before the Planck data release, in Refs. [65–67].

[8] Let us note that there was already a tension between LGC data and pre-Planck CMB data and the sterile neutrino solution was proposed in Refs. [63, 77]

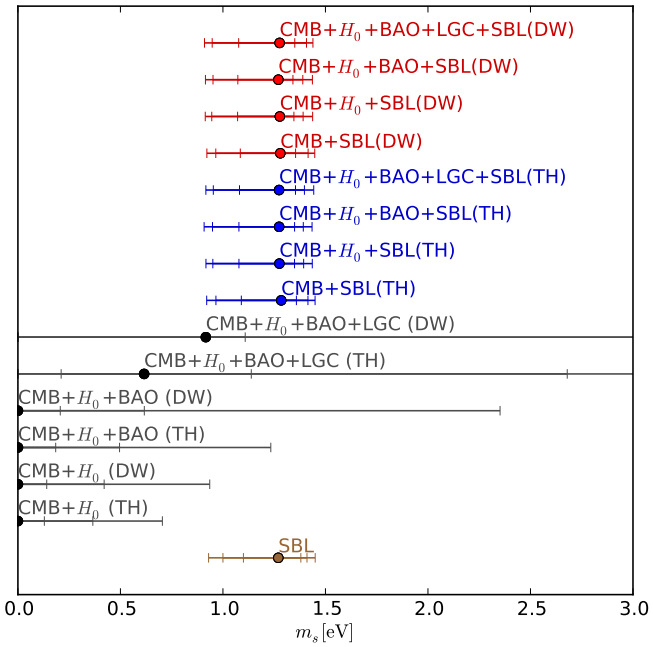


FIG. 4. Comparison of the allowed interval of m_s obtained from the 3+1 analysis of SBL data [30] with those obtained in the fits presented in this paper. The segments in each bar correspond to 68%, 95% and 99% probability. The out-of-bounds upper limits obtained in the CMB+H_0+BAO+LGC analysis are: 7.4 eV (99%, TH), 4.8 eV (95%, DW), 17.1 eV (99%, DW).

Figs. 1, 2, 3, 4 and Tabs. I, II, III confirm this expectation. In particular, from the allowed intervals of m_s in Tab. III and Fig. 4 one can see that the tension between cosmological data and SBL 3+1 oscillations disappears with the inclusion of LGC data.

In the following section we analyze the cosmological data using as prior distribution for m_s the distribution obtained from the analysis of SBL data. This is perfectly consistent in the case of CMB+H_0+BAO+LGC cosmological data. However, we present also the results obtained with the CMB, CMB+H_0 and CMB+H_0+BAO cosmological data, in spite of the tension with SBL data discussed above, because we think that one cannot dismiss the results of laboratory experiments on the basis of cosmological observations, whose interpretation has larger uncertainties.

III. SBL PRIOR

The existence of light sterile neutrinos has been considered in recent years as a plausible possibility motivated by the measurements of anomalies which can be explained by short-baseline (SBL) neutrino oscillations generated by a squared-mass difference of the order of 1 eV^2: the reactor anomaly [25, 78, 79], the Gallium anomaly [24, 27] and the LSND anomaly [80]. Here we consider the results of the analysis of SBL data in the framework of 3+1 mixing presented in Ref. [30]. Following Refs. [40–42], we use the posterior distribution of $m_s \simeq m_4 \simeq \sqrt{\Delta m^2_{41}}$ obtained from the analysis of SBL data as a prior in the `CosmoMC` analysis of cosmological data. The range of m_s allowed by the analysis of SBL data [30] is shown in Fig. 4 and Tab. III. Note that the SBL prior on m_s has different cosmological implications in the thermal and Dodelson-Widrow models, because the $\Delta N_{\rm eff}$ dependence of the effective mass $m_s^{\rm eff}$ is different (see Eqs. (3) and (4)).

Figure 5 shows the results of the analysis of CMB, CMB+H_0, CMB+H_0+BAO and CMB+H_0+BAO+LGC data with the SBL prior in the thermal model. For convenience, the effect of the SBL prior on the allowed regions in the $m_s^{\rm eff}$–$N_{\rm eff}$ plane is illustrated clearly in Fig. 7, where each panel shows the change of the allowed regions due to the inclusion of the SBL prior corresponding to the analysis of the indicated data set. One can see that in all four analyses the SBL prior forces the allowed region in an area near the dashed line which corresponds to $m_s = 1$ eV. In order to keep m_s at the eV scale without increasing too much $m_s^{\rm eff}$, which is forbidden by the cosmological data, $N_{\rm eff}$ is forced towards low values.

In the case of the CMB+H_0+BAO+LGC cosmological data set the addition of the SBL prior approximately confirms the allowed range of $m_s^{\rm eff}$ (see Fig. 3 and Tab. III), but requires a lower $N_{\rm eff}$ (see Fig. 2 and Tab. II), which must be smaller than about 3.7 with 99% probability. As discussed in Ref. [35], in the standard cosmological scenario active-sterile neutrino oscillations generated by values of the mixing parameters allowed by the fit of SBL data imply $\Delta N_{\rm eff} = 1$. Therefore, it is likely that the compatibility of the neutrino oscillation explanation of the SBL anomalies with cosmological data requires that active-sterile neutrino oscillations in the early Universe are somewhat suppressed by a non-standard mechanism, as, for example, a large lepton asymmetry [36–39].

As one can see from Figs. 2, 3, 6 and 7 and from Tabs. II and III, similar conclusions are reached in the Dodelson-Widrow model. One can note, however, that in this case slightly larger values of $N_{\rm eff}$ are allowed with respect to the thermal case, and there is a slightly better compatibility of cosmological and SBL data. This happens because for a given value of m_s given mainly by SBL data and an upper bound on $m_s^{\rm eff}$ given by cosmological data slightly larger values of $\Delta N_{\rm eff} \leq 1$ are allowed by Eq. (4) in the Dodelson-Widrow model than by Eq. (3) in the thermal model.

IV. CONCLUSIONS

In this paper we have analyzed the most recent cosmological data, including those of the Planck experiment [1, 2], taking into account the possible existence of a sterile neutrino with a mass m_s in the eV range, which could

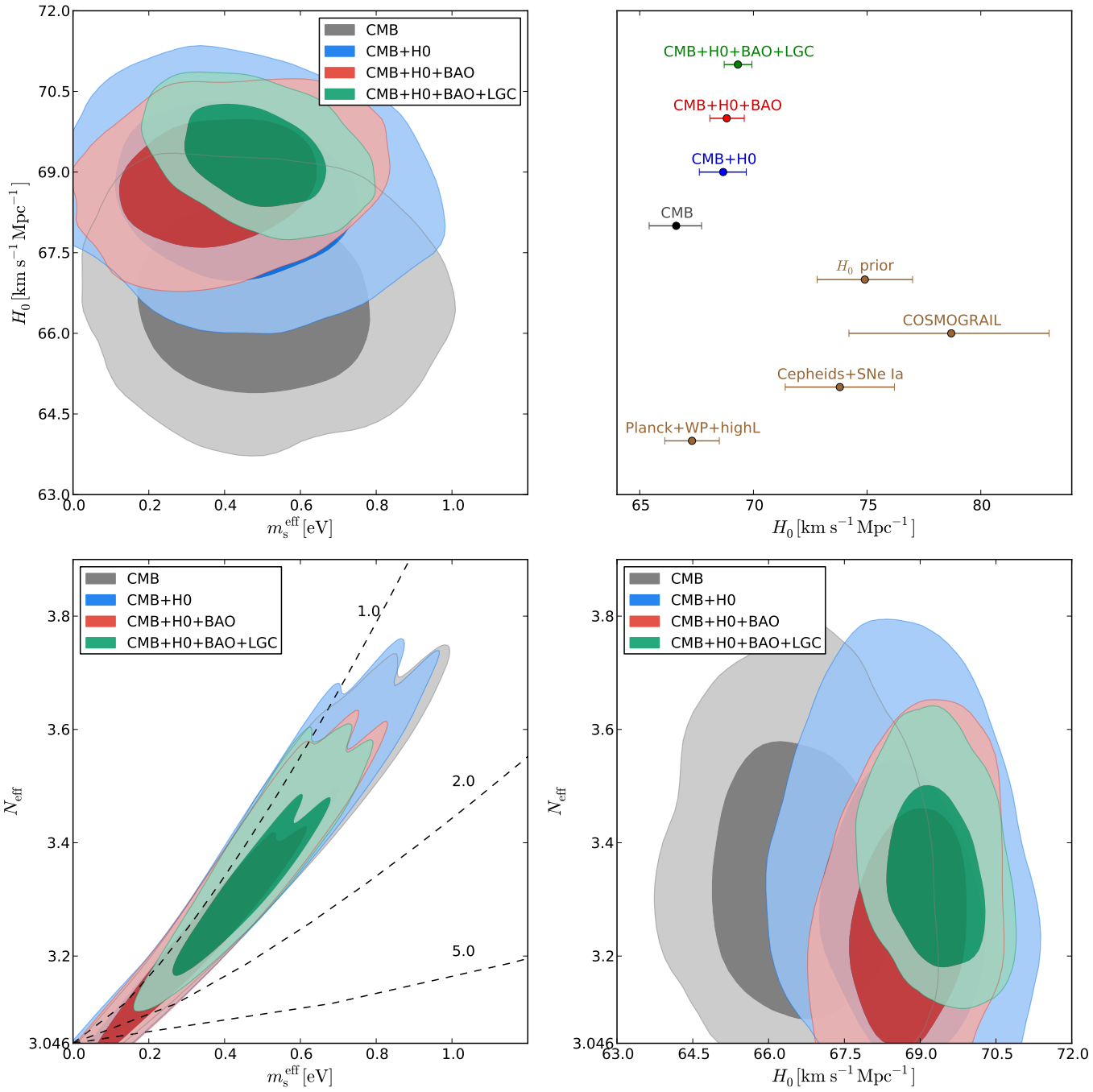


FIG. 5. Results of the analysis of cosmological data with the SBL prior in the thermal model. The light and dark shadowed regions in the 2D plots show, respectively, the 68% and 95% marginalized posterior probability regions obtained from the analysis of the data sets indicated in the legends with corresponding color. In the bottom-left panel m_s is constant along the dashed lines, with the indicated value in eV. The four lower intervals of H_0 in the upper-right panel are equal to those in Fig. 1. In all panels the labels CMB, CMB+H_0, CMB+H_0+BAO and CMB+H_0+BAO+LGC indicate the fits performed in this work.

have the effect of dark radiation in the early Universe. We investigated three effects: 1) the contribution of local measurements of the Hubble constant H_0; 2) the effect of the measurements of the mass distribution of local galaxy clusters [12]; 3) the assumption of a prior distribution for m_s obtained from the analysis of short-baseline oscillation data in the framework of 3+1 mixing, which requires a sterile neutrino mass between about 0.9 and 1.5 eV [30]. For the statistical distribution of the sterile neutrinos we considered the two most studied cases: the thermal model and the Dodelson-Widrow model [34].

We have shown that the local measurements of the Hubble constant H_0 induce an increase of the value of the effective number of relativistic degrees of freedom $N_{\rm eff}$ above the Standard Model value. This is an indication in favor of the existence of sterile neutrinos and their contribution to dark radiation. However, we obtained that the sterile neutrino mass has a 2σ upper bound of about 0.5 eV in the thermal model and about 0.6 eV in the Dodelson-Widrow model. Hence, there is a tension between cosmological and SBL data. The Dodelson-Widrow model is slightly more compatible with SBL data and it may turn out that it is favorite if SBL oscillations will be confirmed by future experiments[9] (see Refs. [21, 68–74]).

The tension between cosmological and SBL data disappears if we consider also the measurements of the local galaxy cluster mass distribution, which favor the existence of sterile neutrinos with eV-scale masses which can suppress the small-scale clustering of galaxies through free-streaming [12]. In this case we obtained a cosmologically allowed range for the sterile neutrino mass which at 2σ can be as large as about 2.7 eV in the thermal model and 4.8 eV in the Dodelson-Widrow model.

In the combined fit of cosmological and SBL data the sterile neutrino mass is restricted around 1 eV by the SBL prior and the cosmological limits on the sterile neutrino mass $m_s^{\rm eff}$ imply that the contribution of the sterile neutrino to the effective number of relativistic degrees of freedom $N_{\rm eff}$ is likely to be smaller than one. In this case, the production of sterile neutrinos in the early Universe must be somewhat suppressed by a non-standard mechanism, as, for example, a large lepton asymmetry [36–39]. The slightly smaller suppression required by the Dodelson-Widrow model and the slightly better compatibility of cosmological and SBL data in this model may be indications in its favor, with respect to the thermal model.

[1] Planck, P. A. R. Ade *et al.*, arXiv:1303.5062.
[2] Planck, P. A. R. Ade *et al.*, arXiv:1303.5076.
[3] T. D. Jacques, L. M. Krauss, and C. Lunardini, Phys.Rev. **D87**, 083515 (2013), arXiv:1301.3119.
[4] P. Di Bari, S. F. King, and A. Merle, Phys.Lett. **B724**, 77 (2013), arXiv:1303.6267.
[5] C. Boehm, M. J. Dolan, and C. McCabe, JCAP **1308**, 041 (2013), arXiv:1303.6270.
[6] C. Kelso, S. Profumo, and F. S. Queiroz, Phys.Rev. **D88**, 023511 (2013), arXiv:1304.5243.
[7] E. D. Valentino, A. Melchiorri, and O. Mena, JCAP **1311**, 018 (2013), arXiv:1304.5981.
[8] N. Said, E. D. Valentino, and M. Gerbino, Phys.Rev. **D88**, 023513 (2013), arXiv:1304.6217.
[9] S. Weinberg, Phys.Rev.Lett. **110**, 241301 (2013), arXiv:1305.1971.
[10] L. Verde, P. Protopapas, and R. Jimenez, arXiv:1306.6766.
[11] L. Verde, S. M. Feeney, D. J. Mortlock, and H. V. Peiris, JCAP **1309**, 013 (2013), arXiv:1307.2904.
[12] M. Wyman, D. H. Rudd, R. A. Vanderveld, and W. Hu, arXiv:1307.7715.
[13] J. Hamann and J. Hasenkamp, JCAP **1310**, 044 (2013), arXiv:1308.3255.
[14] R. A. Battye and A. Moss, arXiv:1308.5870.
[15] C. Giunti and C. W. Kim, *Fundamentals of Neutrino Physics and Astrophysics* (Oxford University Press, Oxford, UK, 2007), ISBN 978-0-19-850871-7.
[16] J. Lesgourgues and S. Pastor, Adv. High Energy Phys. **2012**, 608515 (2012), arXiv:1212.6154.
[17] J. Lesgourgues, G. Mangano, G. Miele, and S. Pastor, *Neutrino Cosmology* (Cambridge University Press, 2013), ISBN: 9781139012874.
[18] G. Mangano, G. Miele, S. Pastor, and M. Peloso, Phys. Lett. **B534**, 8 (2002), astro-ph/0111408.
[19] G. Mangano *et al.*, Nucl. Phys. **B729**, 221 (2005), hep-ph/0506164.
[20] M. C. Gonzalez-Garcia and M. Maltoni, Phys. Rept. **460**, 1 (2008), arXiv:0704.1800.
[21] K. N. Abazajian *et al.*, arXiv:1204.5379.
[22] A. Palazzo, Mod.Phys.Lett. **A28**, 1330004 (2013), arXiv:1302.1102.
[23] M. Drewes, International Journal of Modern Physics E, Vol. **22**, 1330019 (2013), arXiv:1303.6912.
[24] C. Giunti and M. Laveder, Phys. Rev. **C83**, 065504 (2011), arXiv:1006.3244.
[25] G. Mention *et al.*, Phys. Rev. **D83**, 073006 (2011), arXiv:1101.2755.
[26] J. Conrad, C. Ignarra, G. Karagiorgi, M. Shaevitz, and J. Spitz, Adv.High Energy Phys. **2013**, 163897 (2013), arXiv:1207.4765.
[27] C. Giunti, M. Laveder, Y. Li, Q. Liu, and H. Long, Phys. Rev. **D86**, 113014 (2012), arXiv:1210.5715.
[28] C. Giunti, M. Laveder, Y. Li, and H. Long, Phys. Rev. **D87**, 013004 (2013), arXiv:1212.3805.
[29] J. Kopp, P. A. N. Machado, M. Maltoni, and T. Schwetz, JHEP **1305**, 050 (2013), arXiv:1303.3011.
[30] C. Giunti, M. Laveder, Y. Li, and H. Long, Phys.Rev. **D88**, 073008 (2013), arXiv:1308.5288.
[31] Z. Hou, R. Keisler, L. Knox, M. Millea, and C. Reichardt, Phys.Rev. **D87**, 083008 (2013), arXiv:1104.2333.

[9] The existence of sterile neutrinos with eV-scale masses can be tested also in β-decay [27, 28, 81–84] and neutrinoless double-β decay experiments [27, 28, 85–89].

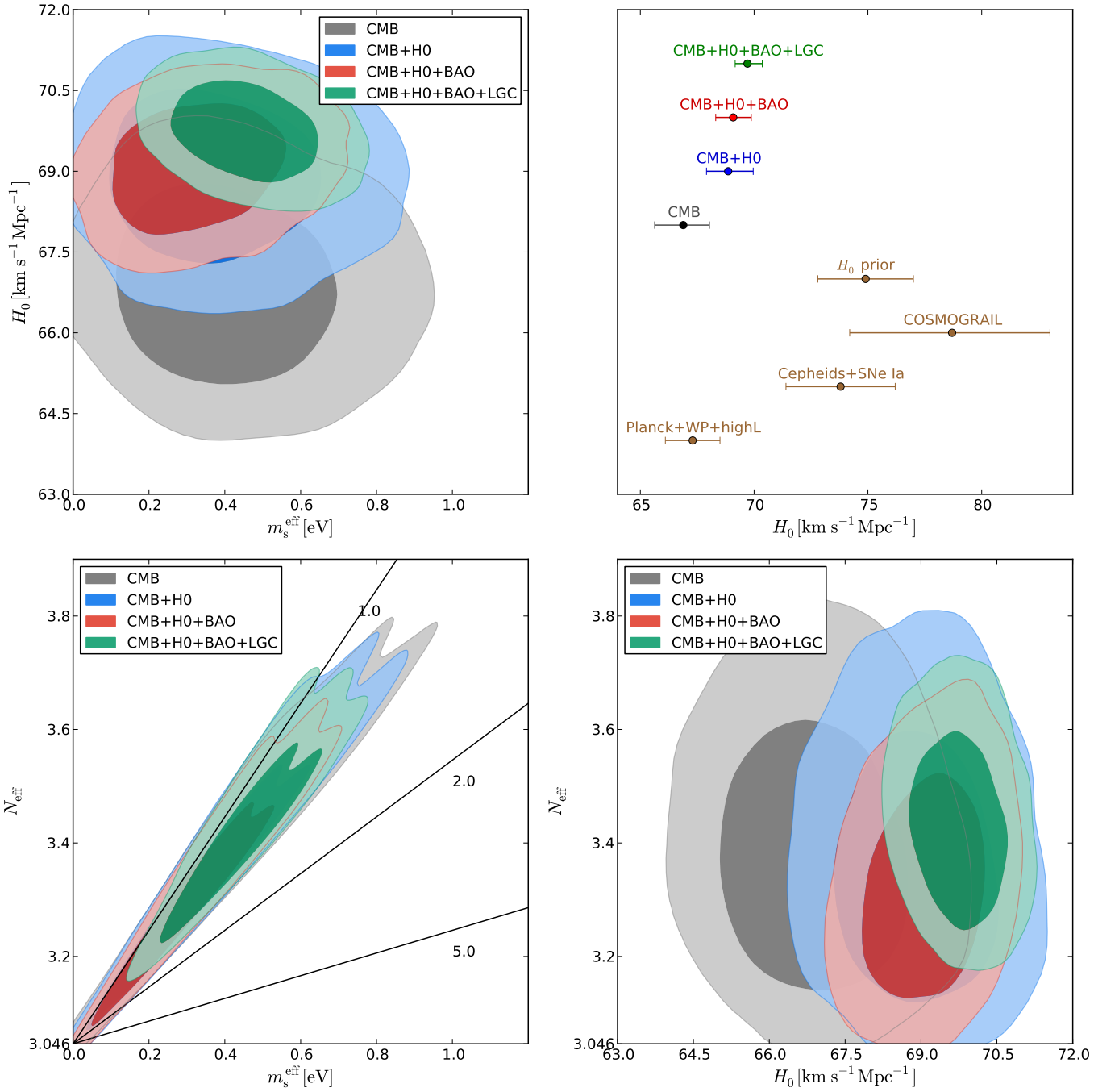


FIG. 6. Results of the analysis of cosmological data with the SBL prior in the Dodelson-Widrow model. The light and dark shadowed regions in the 2D plots show, respectively, the 68% and 95% marginalized posterior probability regions obtained from the analysis of the data sets indicated in the legends with corresponding color. In the bottom-left panel m_s is constant along the solid lines, with the indicated value in eV. The four lower intervals of H_0 in the upper-right panel are equal to those in Fig. 1. In all panels the labels CMB, CMB+H_0, CMB+H_0+BAO and CMB+H_0+BAO+LGC indicate the fits performed in this work.

[32] M. Archidiacono, E. Giusarma, S. Hannestad, and O. Mena, arXiv:1307.0637.
[33] M. A. Acero and J. Lesgourgues, Phys. Rev. **D79**, 045026 (2009), arXiv:0812.2249.
[34] S. Dodelson and L. M. Widrow, Phys. Rev. Lett. **72**, 17 (1994), hep-ph/9303287.
[35] A. Mirizzi *et al.*, Phys. Lett. **B726**, 8 (2013), arXiv:1303.5368.
[36] S. Hannestad, I. Tamborra, and T. Tram, JCAP **1207**, 025 (2012), arXiv:1204.5861.
[37] A. Mirizzi, N. Saviano, G. Miele, and P. D. Serpico, Phys.Rev. **D86**, 053009 (2012), arXiv:1206.1046.
[38] N. Saviano *et al.*, Phys.Rev. **D87**, 073006 (2013), arXiv:1302.1200.
[39] S. Hannestad, R. S. Hansen, and T. Tram, JCAP **1304**, 032 (2013), arXiv:1302.7279.
[40] M. Archidiacono, N. Fornengo, C. Giunti, and A. Melchiorri, Phys. Rev. **D86**, 065028 (2012), arXiv:1207.6515.
[41] M. Archidiacono, N. Fornengo, C. Giunti, S. Hannestad, and A. Melchiorri, Phys.Rev. **D87**, 125034 (2013), arXiv:1302.6720.
[42] J. R. Kristiansen, O. Elgaroy, C. Giunti, and M. Laveder, arXiv:1303.4654.
[43] A. G. Riess *et al.*, Astrophys.J. **730**, 119 (2011), arXiv:1103.2976.
[44] S. Suyu *et al.*, Astrophys.J. **766**, 70 (2013), arXiv:1208.6010.
[45] A. Lewis and S. Bridle, Phys. Rev. **D66**, 103511 (2002), astro-ph/0205436.
[46] A. Lewis, A. Challinor, and A. Lasenby, Astrophys.J. **538**, 473 (2000), astro-ph/9911177.
[47] Planck, Planck, arXiv:1303.5075.
[48] WMAP, C. L. Bennett *et al.*, Astrophys.J.Suppl. **208**, 20 (2013), arXiv:1212.5225.
[49] S. Das *et al.*, arXiv:1301.1037.
[50] R. Keisler *et al.*, Astrophys. J. **743**, 28 (2011), arXiv:1105.3182.
[51] C. Reichardt *et al.*, Astrophys.J. **755**, 70 (2012), arXiv:1111.0932.
[52] J. Dunkley *et al.*, arXiv:1301.0776.
[53] WMAP, G. Hinshaw *et al.*, Astrophys.J.Suppl. **208**, 19 (2013), arXiv:1212.5226.
[54] B. A. Bassett and R. Hlozek, arXiv:0910.5224.
[55] SDSS, K. N. Abazajian *et al.*, Astrophys.J.Suppl. **182**, 543 (2009), arXiv:0812.0649.
[56] SDSS, W. J. Percival *et al.*, Mon.Not.Roy.Astron.Soc. **401**, 2148 (2010), arXiv:0907.1660.
[57] N. Padmanabhan *et al.*, Mon.Not.Roy.Astron.Soc. **427**, 2132 (2012), arXiv:1202.0090.
[58] SDSS, C. P. Ahn *et al.*, Astrophys.J.Suppl. **203**, 21 (2012), arXiv:1207.7137.
[59] L. Anderson *et al.*, Mon.Not.Roy.Astron.Soc. **428**, 1036 (2013), arXiv:1203.6594.
[60] F. Beutler *et al.*, Mon.Not.Roy.Astron.Soc. **416**, 3017 (2011), arXiv:1106.3366.
[61] D. H. Jones *et al.*, arXiv:0903.5451.
[62] A. Vikhlinin *et al.*, Astrophys. J. **692**, 1060 (2009), arXiv:0812.2720.
[63] R. Burenin and A. Vikhlinin, arXiv:1202.2889.
[64] W. L. Freedman *et al.*, Astrophys.J. **758**, 24 (2012), arXiv:1208.3281.
[65] E. Giusarma, M. Archidiacono, R. de Putter, A. Melchiorri, and O. Mena, Phys. Rev. **D85**, 083522 (2012), arXiv:1112.4661.
[66] H. Motohashi, A. A. Starobinsky, and J. Yokoyama, Phys.Rev.Lett. **110**, 121302 (2013), arXiv:1203.6828.
[67] C. M. Ho and R. J. Scherrer, Phys.Rev. **D87**, 065016 (2013), arXiv:1212.1689.
[68] M. Cribier *et al.*, Phys. Rev. Lett. **107**, 201801 (2011), arXiv:1107.2335.
[69] A. Bungau *et al.*, Phys.Rev.Lett. **109**, 141802 (2012), arXiv:1205.4419.
[70] C. Rubbia, A. Guglielmi, F. Pietropaolo, and P. Sala, arXiv:1304.2047.
[71] Borexino, G. Bellini *et al.*, JHEP **1308**, 038 (2013), arXiv:1304.7721.
[72] OscSNS, M. Elnimr *et al.*, arXiv:1307.7097.
[73] X. Qian, C. Zhang, M. Diwan, and P. Vogel, arXiv:1308.5700.
[74] nuSTORM, D. Adey *et al.*, arXiv:1308.6822.
[75] W. Hu and B. Jain, Phys.Rev. **D70**, 043009 (2004), astro-ph/0312395.
[76] W. Hu, ASP Conf.Ser. **339**, 215 (2005), astro-ph/0407158.
[77] R. A. Burenin, Astron.Lett. **39**, 357 (2013), arXiv:1301.4791.
[78] T. A. Mueller *et al.*, Phys. Rev. **C83**, 054615 (2011), arXiv:1101.2663.
[79] P. Huber, Phys. Rev. **C84**, 024617 (2011), arXiv:1106.0687.
[80] LSND, A. Aguilar *et al.*, Phys. Rev. **D64**, 112007 (2001), hep-ex/0104049.
[81] A. S. Riis and S. Hannestad, JCAP **1102**, 011 (2011), arXiv:1008.1495.
[82] A. S. Riis, S. Hannestad, and C. Weinheimer, Phys. Rev. **C84**, 045503 (2011), arXiv:1105.6005.
[83] J. A. Formaggio and J. Barrett, Phys. Lett. **B706**, 68 (2011), arXiv:1105.1326.
[84] A. Esmaili and O. L. G. Peres, Phys. Rev. **D85**, 117301 (2012), arXiv:1203.2632.
[85] J. Barry, W. Rodejohann, and H. Zhang, JHEP **07**, 091 (2011), arXiv:1105.3911.
[86] Y. Li and S. Liu, Phys. Lett. **B706**, 406 (2012), arXiv:1110.5795.
[87] C. Giunti and M. Laveder, Phys. Lett. **B706**, 200 (2011), arXiv:1111.1069.
[88] W. Rodejohann, J. Phys. **G39**, 124008 (2012), arXiv:1206.2560.
[89] I. Girardi, A. Meroni, and S. T. Petcov, arXiv:1308.5802.

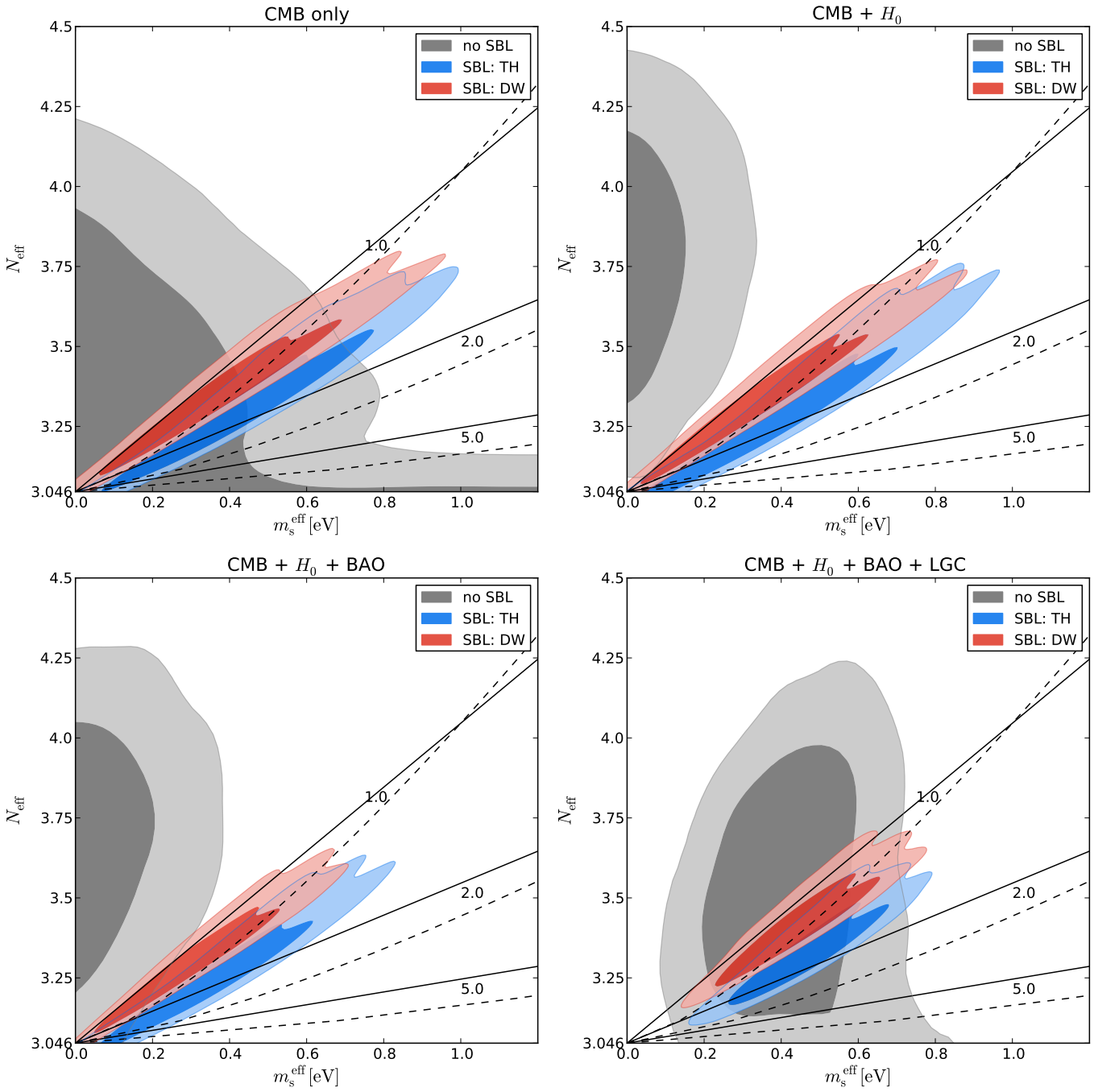


FIG. 7. Illustrations of the effect of the SBL prior on the results of the fits of CMB, CMB+H_0, CMB+H_0+BAO and CMB+H_0+BAO+LGC data. The value of m_s is constant, with the indicated value in eV, along the dashed lines in the thermal model and along the solid lines in the Dodelson-Widrow model.